Alpenglow: Binghamton University Undergraduate Journal of Research and Creative Activity

Volume 3 | Issue 1 Article 7

4-25-2017

The Applicability of Short-Wave Infrared (SWIR) Imagery for Archaeological Landscape Classification on Rapa Nui (Easter Island), Chile

Dylan S. Davis
Binghamton University--SUNY, ddavis17@binghamton.edu

Abstract
High-resolution multispectral imagery provides an effective means for measuring the archaeological record of Rapa Nui. Previous work has suggested that the island's prehistoric cultivation features known as "lithic mulch gardens" can be identified using near infrared imagery (NIR). Lithic mulching was a laborious but critical strategy for prehistoric populations who relied on cultivating sweet potato and taro in nutrient poor soils for their subsistence. The new WorldView-3 satellite offers researchers access to short-wave infrared (SWIR) bands, imagery that provides additional information about moisture content and mineral composition. While these bands should provide a better means for identifying lithic mulch gardens, this new imagery is currently only available at a lower spatial resolution than NIR images (7.5 m vs. 1.24 m). Here, I evaluate whether these lower-resolution SWIR images can be used for identifying "lithic mulch garden" features despite their resolution difference. Comparing the results of SWIR imagery with that of previous analyses reveals markedly similar classification accuracy despite having the lower spatial resolution. This result suggests that SWIR may provide a new tool for researchers interested in questions of prehistoric land-use that will become increasingly more powerful as greater spatial resolutions become available.

Introduction

Identifying prehistoric land-use patterns is one major focus of archaeological inquiry that has gained popularity in recent years due to advancements in remote sensing technologies. Analyzing the ways in which environments are transformed by people is an important marker of the structure and function of local communities (Reitz, et al., 2008 p. 12). On Rapa Nui, environmental limitations such as low soil nutrients and a lack of flowing water sources demanded agricultural innovation (Stevenson, et al., 2002, p. 18). One of the ways in which this was accomplished was through the process of "lithic mulching" (see Wozniak, 1999, 2003). Recenttudies of such activity have been undertaken utilizing multispectral imagery.

These studies have shown that remote sensing technology can be of great assistance in advancing archaeological knowledge. Satellite image analysis has allowed for the identification of many previously unknown sites, and has been used to monitor the state of preservation for many archaeological areas (Parcak, et al., 2016; Parcak, 2009). Remote sensing has often been utilized to track environmental and landscape changes, especially in terms of biophysical information, such

as agricultural monitoring and moisture content differentiation (Jensen, 2007, p. 355). On Rapa Nui, remote sensing is a fundamental tool in mapping the island's landscape and identifying archaeological features (see Bradford, 2005; Bradford, et al., 2005; Flaws, 2010; Ladefoged, et al., 2013; Lipo & Hunt, 2005; Morrison, 2012).

Remote sensing has been used on Rapa Nui by archaeologists in order to map the extent of "lithic mulching" activity throughout the island. Past studies (e.g. Flaws, 2010; Ladefoged, et al., 2013) have made use of high resolution NIR imagery to identify rock gardens, and have demonstrated that the highest densities of such landscape modifications occur close to the coast. However, such studies have resulted in a substantial amount of misclassification (~25-35%), which, as this study aims to prove, can be attributed to the unavailability of SWIR imagery.

In this paper, high resolution satellite imagery (WorldView-3) is utilized to identify landscape features such as lithic mulching. WorldView-3 has slightly higher spatial resolution than WorldView-2, and includes 8 bands of short-wave infrared (SWIR), which reveal additional information about mineral composition and soil moisture. The results of near infrared (NIR) and SWIR image classifications are compared in their ability to distinguish between landscape features. Overall, it is the goal of this article to highlight the benefits of SWIR imagery by comparing the accuracy of SWIR and NIR image classifications in their ability to distinguish between archaeological features and components of the natural landscape.

Land-use on Rapa Nui

Rapa Nui is a small island (164 km^2) in the middle of the Pacific Ocean, 3200 kilometers from the coast of South America. The island is isolated, containing few resources, and has shallow, rocky soils that are extremely well drained and lacking in nutrients (Louwagie, et al., 2006, p.

292). The pre-human landscape was largely covered in thick forests and approximately 20 other species of flora (Mann, et al., 2008, p. 17; Mieth & Bork, 2015, p. 95). Through the 13th century the *Jubaea* palm dominated the landscape, but after Polynesian arrival on Rapa Nui, the dense palm woodlands were quickly deforested through burning and rat infestations (Basner, et al., 2008; Hunt, 2007; Mann, et al., 2008, p. 17; Mieth, et al., 2002, p. 92).

Upon human arrival on Rapa Nui, transformation of the landscape was nearly immediate. As noted by Rainbird (2002, p. 443), prehistory in the Pacific is underscored by a link between human settlement and environmental manipulation. Crops were cultivated in agricultural gardens and local inhabitants soon coalesced, often under unified ceremonial beliefs and genealogical ties (Fischer, 2005, p. 21; Martinsson-Wallin & Wallin, 2014, p. 325; Sahlins, 1955, p. 1037; Stevenson, et al., 2006, pp. 919-920).This pattern is not unique to Polynesia, and is indeed found ubiquitously in archaeological records across the world.

A multitude of archaeological investigations reveal that a large majority of Rapa Nui is covered in rock gardens, which in the past were used for intensive cultivation (Bork, et al., 2002; Flaws, 2010; Horrocks & Wozniak, 2008, p. 141; Ladefoged, et al., 2013; Stevenson, 1999; Wozniak, 1999, 2003). Lithic mulching allows for the protection of crops from prolonged winds, erosion, and temperature variability (Lightfoot, 1994, pp. 172-173). Rock gardens, known as *manavai*, were also constructed and provided wind protection, stable diurnal temperatures, and improved soil nutrients (Bork, et al., 2004, p. 10; Ladefoged, et al., 2010, p. 82; Stevenson, et al., 2002, p. 19; Wozniak, 1999, p. 98). Wozniak (1999, p. 96) considers lithic mulching technology to be one of the most important innovations made by the prehistoric inhabitants of Rapa Nui. It must be noted however, that lithic mulching only provides slight improvements in soil quality, and

these improvements would only have been noticeable during periods of extreme drought or in crops that are grown in suboptimal locations (Louwagie, et al., 2006, p. 307).

Stones are a ubiquitous aspect of the Rapa Nui landscape; according to Bork et al. (2004, p. 12), as much as 76 km^2 of the island's surface are covered in mulching stones. Hamilton et al. (2011) view stones as a key element of the Rapa Nui landscape (p. 186). On an island composed of stone, it is necessary to determine which stones are altered by humans, and which are simply unaltered components of the natural landscape. This task is attempted using high resolution multispectral satellite imagery.

Remote sensing has been used as a tool for mapping the landscape of Rapa Nui, and determining where archaeological features are present throughout the island. In his MA Thesis, Andrew Flaws (2010, p. 35) uses WorldView-2 NIR multispectral imagery and maximum likelihood classification (MLC) to identify rock gardening throughout Rapa Nui, and determines that supervised classification yields an overall accuracy of 65%. In addition to mapping the locations with the highest density of rock gardening, Flaws (2010, p. 49) also determines that lithic mulching is rare in elevations above 350 meters. Flaw's conclusions about lithic mulch distribution are important, but may be inaccurate due to the fact that his accuracy assessment revealed that as much as 35% of his land classification was inaccurate when checked by a ground-truth image.

In a study by Ladefoged et al. (2013, p. 1211), WorldView-2 NIR imagery is also used to identify lithic mulching, and classification yields mixed results ranging from 55% to 74% accuracy. The authors do claim that in some areas, there is "a good deal" of misclassification (Ladefoged, et al., 2013, p. 1208). Once again, the shortfalls of a purely NIR based remote sensing study for the purposes of identifying rock-features is illustrated. Utilizing the SWIR bands of the electromagnetic spectrum allow for more accurate delineation between rock and mineral types,

and will likely provide greater accuracy in classifying Rapa Nui's landscape. It is the goal of this study to assess this hypothesis.

Short-Wave Infrared

Remote sensing offers an unparalleled glimpse at large portions of a given landscape, and the ability to view landscapes in parts of the electromagnetic spectrum that are invisible to the naked eye. The electromagnetic spectrum is often divided into specific wavelengths (or bands) to identify specific physical features (Jenson, 2007, pp. 41-42). Each band in the electromagnetic spectrum, when recorded by remote sensors, reveals different information about the environment being photographed (see Table 1).

Table 1: Electromagnetic Spectrum with color breakdowns and their respective uses.

Color	Wavelength (nm)	Uses
Blue	450-500	Underwater terrain
Green	500-600	Vegetation monitoring
Red	630-690	Vegetation stress, chlorophyll production
NIR	760-900	Vegetation stress, biomass
SWIR	1000-3000	Moisture content, mineral distinctions

Discrepancies in moisture content and vegetation health can give archaeologists glimpses into the features lying below the surface, such as buried walls and architectural structures (Parcak, 2009, p. 3). For the purposes of Rapa Nui's archaeological landscape, the omnipresence of rocks presents a useful test for SWIR bands in distinguishing between different rock types. WorldView-3 imagery used in this study contains high resolution SWIR bands. The primary hypothesis of this study is that SWIR bands will be successful in classifying the landscape and distinguishing between anthropogenic land cover (lithic mulch) and natural rock formations.

SWIR has been shown to perform better than other intervals of the electromagnetic spectrum in tasks such as minimizing haze, fog, cloud coverage, and smoke (Driggers, et al., 2013).

Studies also show that SWIR imagery provides better estimates of vegetation cover (Gill & Phinn, 2008). In a remote sensing study by Asner and Lobell (2000, p. 104) it is determined the SWIR bands are the "best choice" for separating different types of vegetation and different types of soil. Additionally, Drake et al. (1999, p. 24) conclude that SWIR is extremely useful for mapping different geological components in remote sensing imagery.

All of these studies (i.e. Gill & Phinn, 2008; Asner and Lobell, 2000, and Drake, et al., 1999) were conducted using low resolution satellite imagery such as AVIRIS (Airborne Visible / Infrared Imaging Spectrometer) and ASTER (Advanced Spaceborne Thermal Emission and Reflection Radiometer). Prior to the launch of WorldView-3 in 2014, SWIR was limited to lower resolution imagery (i.e. 30 m.) from satellites such as ASTER (Jenson, 2007, p. 231). The SWIR sensors on WorldView-3 have a resolution of 3.7 meters (7.5 meters for commercial use), and are at a much higher resolution than ASTER satellite imagery. Thus, the goal of this study is to assess whether or not high resolution (7.5 m) SWIR imagery is comparable to high resolution (1.24 m) NIR in identifying different land-cover types on Rapa Nui, specifically pertaining to lithic mulching and soil moisture.

Materials and Methods

For this study, WorldView-3 satellite imagery was analyzed and processed using ArcGIS 10.2. The image covers an area of 23.7 km^2 on the northwest coast of Rapa Nui (see Figure 1) and contains an area of known lithic mulching activity. The NIR and SWIR bands were each analyzed and classified using unsupervised and supervised classification. Unsupervised classification is conducted purely by computer algorithms, and the analyst must then identify the different classes identified by cross-checking them with ground-truth images. Supervised classification is

conducted by the analyst, who chooses the classes and identifies a sample of pixels that belong in each class. Accuracy tests were then implemented to determine the overall success of each supervised classification. All maps use the WGS 84 coordinate reference system to avoid locational displacement (see Vargas, et al., 2007).

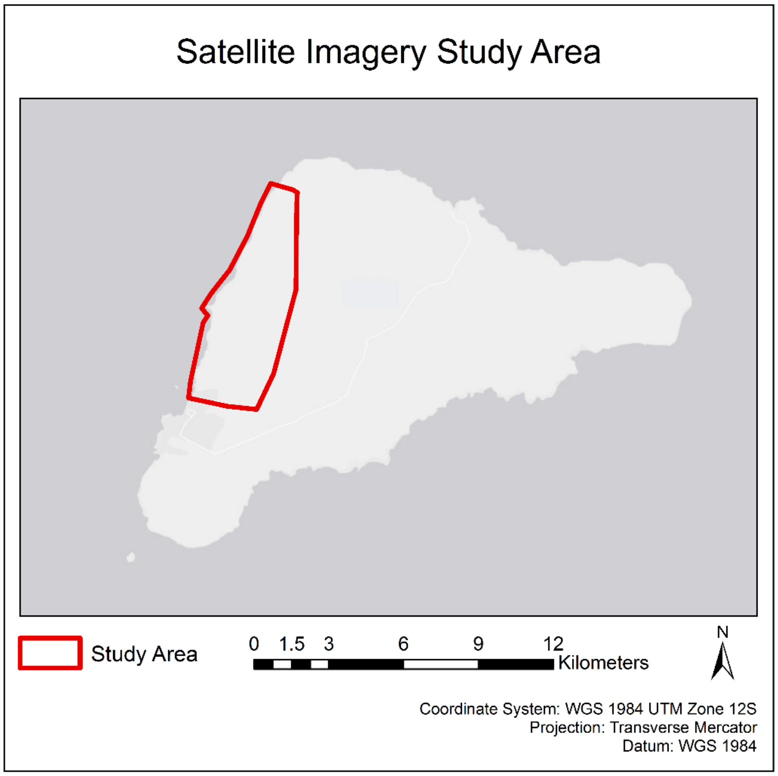

Figure 1: Map showing the boundaries of the satellite imagery and the study area. The study area comprises of 23.7 km^2, which makes up approximately 14.5% of Rapa Nui's total land area.

WorldView-3

WorldView-3 is a satellite that was launched in 2014, and records extremely high spatial resolution imagery. It has an orbital period of 97 minutes and its temporal resolution is 1-4.5 days (Maglione, 2016, p. 96). The satellite is equipped with a panchromatic band at 0.31 meter spatial resolution, and multispectral bands at 1.24 meter spatial resolution (Digital Globe, 2014). Besides higher resolution, WorldView-3 differs from WorldView-2 in two ways: it has 8 additional bands

of short-wave infrared (SWIR) sensors at 3.7 meter spatial resolution and 12 bands of Clouds, Aerosols, Water Vapor, Ice and Snow (CAVIS) sensors at 30 meter resolution (Longbotham, et al., 2015). The SWIR bands are limited to 7.5 meter spatial resolution for commercial use (Asadzadeh, et al., 2016, p. 163)

WorldView-3 has proven successful at identifying different geological features, including hydrocarbon based materials, such as petroleum (Asadzadeh & de Souza Filho, 2016; Kruse, et al., 2015). In addition to mineral classification, WorldView-3 imagery can be used for other classification tasks, such as agricultural mapping and urban monitoring (Longbotham, et al., 2014). WorldView-3 is a relatively new satellite, and new studies are just beginning to utilize this satellite and its capabilities.

Preliminary Analysis

Using NIR and SWIR bands, WorldView-3 image analysis was undertaken. All image analysis was performed using ArcGIS 10.2. The first step of this analysis consisted of basic visual interpretation, with the intention of determining the image bands that best reveal the areas of interest (i.e. lithic mulch and *manavai*), and provide the best contrast between different features. Comparison between true-color ground images and the multispectral images were consistently made to ensure proper identification of features during this phase of analysis. Lithic mulch and *manavai* are the most distinctly visible in WorldView-3 imagery using composite images of NIR bands 7, 8, and 5 (NIR1, NIR2, Red) and bands 7, 6, and 3 (NIR1, Red Edge, Green) using a histogram equalization stretch. Preliminary image analysis using SWIR shows the best results using bands 5 (2145 - 2185 nm), 2 (1550 - 1590 nm), and 3 (1640 - 1680 nm) with a histogram equalization stretch, and bands 6 (2185 - 2225 nm), 1 (1195 - 1225 nm), and 4 (1710 - 1750 nm) with a percent clip stretch. The contrast between lithic mulching stones and bare ground was

greatest using these band combinations, and therefore provided the best spectral juxtaposition for classification purposes. After initial observations were made and the best composites were determined for this study, image processing commenced.

Land-cover Classification

Land-cover classification is critical for identifying archaeological features because it allows for the landscape to be divided into specific categories, which allow for certain kinds of features to be identified automatically by a computer. As mentioned previously, there are two main types of classification – supervised and unsupervised. In order to best classify the data, both unsupervised and supervised classifications were conducted, and initially compared. Although supervised classification turns out to be more accurate, the unsupervised classification reveals interesting results. All classifications are made on both sets of NIR and SWIR composites.

Iso-cluster unsupervised classification was conducted using 10 class differentiations and a minimum class size of 20 cells. In order to ensure the greatest accuracy, the unsupervised classes underwent class probability testing. Class probability testing reveals some "mixed" classes, which have spectral similarities but medium probabilities (35%-66%) between classes.

Before supervised classification can take place, training samples have to be created to guide ArcGIS in the classification process. Using pan-sharpening, composite images were created by merging the lower resolution NIR and SWIR with the high resolution panchromatic (PAN) imagery. Pan-sharpening is a technique that allows for geometric details of the higher resolution panchromatic image to be integrated into a slightly lower resolution multispectral image (Maglione, 2016, p. 92). Simple mean pan-sharpening is used for the SWIR 614 composite image, and IHS pan-sharpening is used for the NIR 785 composite image. Training samples were drawn around known lithic mulch sites and other noticeable landscape components (see Table 2).

Table 2: Training Samples and their respective pixel count.

Class	**Count**
Moist Soil	7269
Dry Soil	9918
Mulch	7485
Water	189047
Grass	5946
Trees	7197
Bedrock	7208

Following the creation of the training samples, each of the NIR and SWIR composites were classified using Maximum Likelihood Supervised Classification. SWIR manages to show most of the same details (but in a much more pixelated state) as the NIR, with some exceptions (discussed later). After initial analysis and comparisons between the NIR and SWIR supervised classifications were completed, class probability testing was performed on the images. A total of 150 randomly generated points were assigned specific landscape classes (i.e. lithic mulch, water, bedrock, etc.) by comparing each point to true-color imagery. These points were then compared to the classified images and accuracy was assessed. Class probability provides additional information about "mixed classification" that occurs, and the differences between the NIR and SWIR appear to be miniscule according to the class probabilities (See Figure 2).

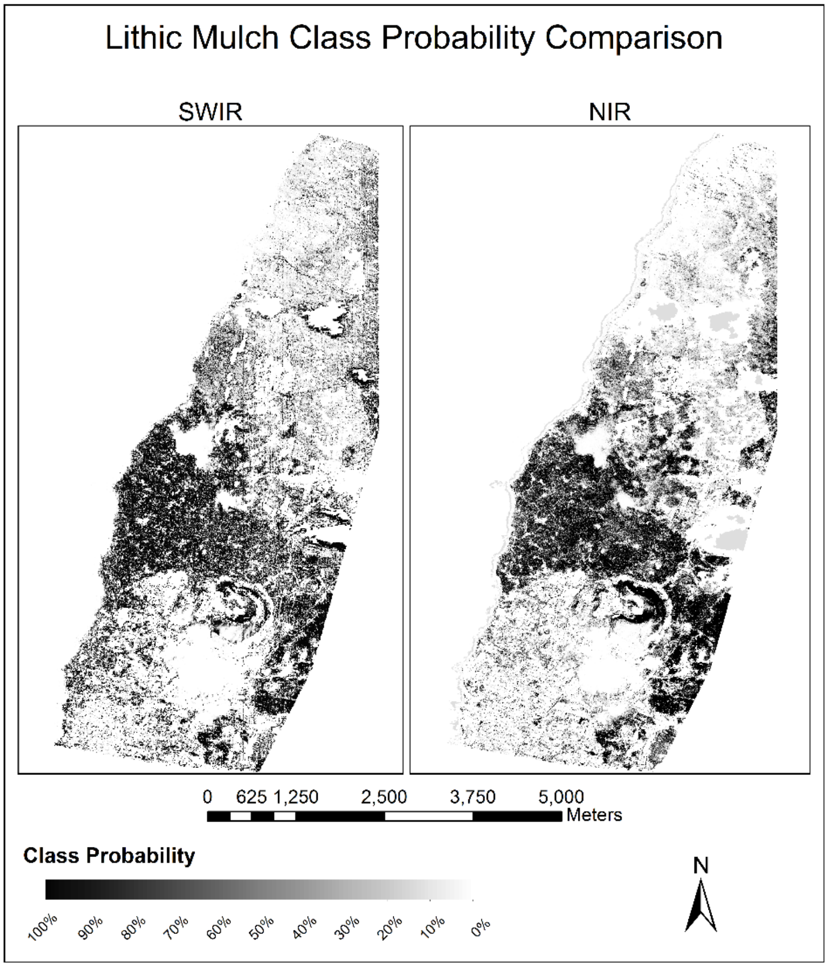

Figure 2: "Mixed" probability results for lithic mulch classification. Overall, the images show a similar pattern, with lithic mulching being most abundant in the south-central section of the image. It is noticeable that the SWIR classification has additional mixing, especially in the northern-most region where bedrock is abundant.

Once the maximum likelihood supervised classification was performed on the NIR and SWIR images, accuracy assessments were conducted using an error matrix. An error matrix is a way in which to assess accuracy of pixel values that are determined based on a classified map and ground data (Kuzera & Pontius Jr., 2008, p. 255). There are many different types of accuracy assessment (e.g. overall accuracy, kappa coefficient, modified kappa, user accuracy, producer accuracy, etc.) but there is no agreement on a standard approach that has been universally adopted by the remote sensing community (Liu, et al., 2007, p. 609). The Kappa coefficient (κ) has been

one of the most widely favored methods of accuracy assessment for many years in the remote sensing field, but has also been criticized for its emphasis on random chance (Pontius Jr. & Millones, 2011; Stehman, 1997). For this reason, additional accuracy tests are used. After error matrices are created, a z-test is utilized to assess the difference in accuracy between the SWIR and NIR classifications.

Results

Unsupervised Classification

When multiple iso-cluster unsupervised classifications were performed using different numbers of classes, and each time, the NIR produced fewer classes than the SWIR. This highlights the increased sensitivity of SWIR imagery to spectral differences. The NIR isocluster does manage to distinguish very well between different levels of moisture (both in vegetation and in soil). Although the resolution is better in the NIR image, SWIR manages to capture nearly identical details, and in some instance (especially in geological differences), the SWIR bands reveal more detail than the NIR bands. Geological patterns are also noticable in the NIR classifications, but this trend is better seen in the SWIR classification.

The SWIR unsupervised classification was extremely keen at picking up on subtle differences in moisture and landscape type. The classifications were compared to true-ground imagery to determine what features were present in each class. For SWIR there are significant variations in ground classification, and class probability testing reveals that lithic mulching varies between different spectral signatures. Additionally, vegetation health can be seen in the SWIR classification, as some cells contain higher and lower moisture content values than others within the same area. Geological patterns are clearly noticable in the SWIR classification, and linear rock patterns indicate past lava flows where bedrock now resides. This trend is also seen in the NIR.

Nonetheless, SWIR picks up on everything that the NIR picks up on, even at a significantly lower spatial resolution (See Figure 3). Nonetheless, there were issues in the accuracy of the unsupervised classifications for both NIR and SWIR, which is seen in the differences between the images in Figure 3.

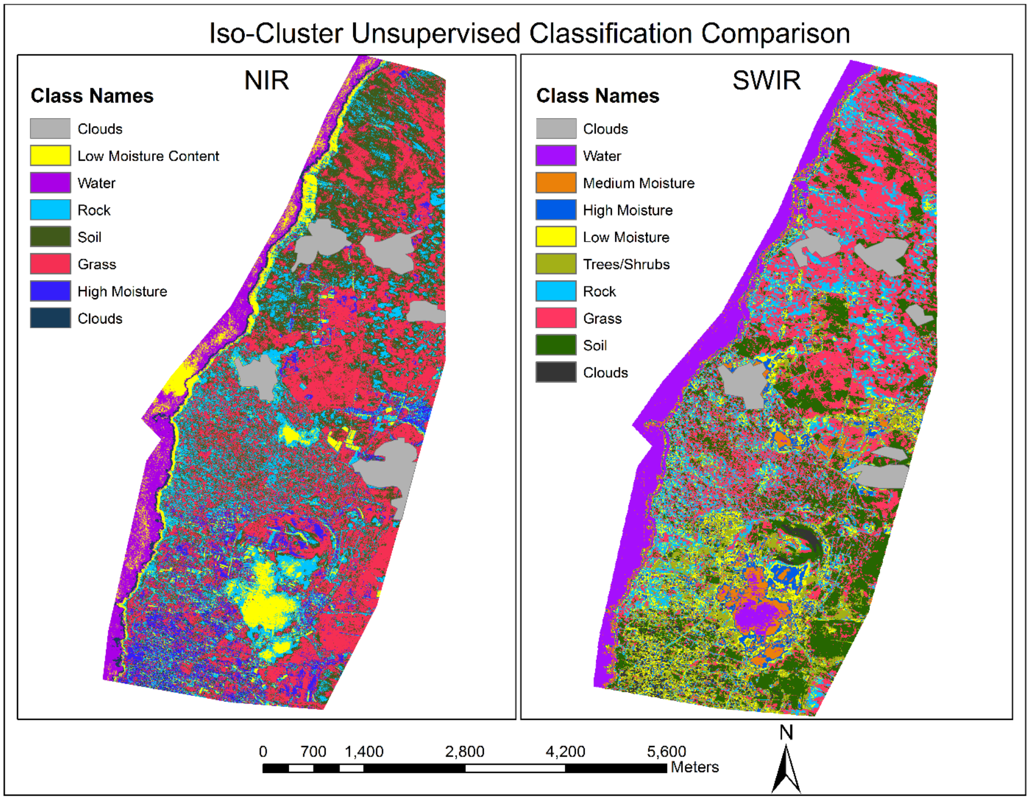

Figure 3. Iso-cluster unsupervised classification proved useful in establishing differences in the geological landscape that were not clearly noticeable using true-color imagery. Notice, in particular, the northernmost part of the image, where SWIR picks up on linear-striations indicating lava-flow marks and natural rock outcrops. This is also seen, but less so, in the NIR image.

The isocluster unsupervised classification of SWIR and NIR allows for differentiations to be made between anthropogenic rock structures and natural rock outcrops. This is noticable in the patterning of rock coverage and its overall surroundings. Lithic mulch is characterized by small rocks surrounded by soils at low-to-high moisture levels. Natural rock formations and bedrock are characterized by large uniform clusters of rock-classified cells, and are usually aligned in a linear pattern, indicating ancient lava flows. Natural rock formations do not seem to retain as much

moisture, and areas that were not manipulated for human use are usually less diverse in terms of classifications within the immediate surroundings. Initially distinguishing between bedrock and lithic mulch is made easier by conducting an isocluster unsupervised classification.

Class probability testing of the unsupervised classifications reveals that many pixels are a “mixed”, with a probability that is midway between two different spectral classes – specifically high moisture content, grass, and bedrock. SWIR waves, even at much lower resolution than NIR, can pick up moisture variations in the lithic mulch and the surrounding soil, thus indicating that moisture content is indeed increased by the mulching technology.

Supervised Classification

Maximum likelihood classification (MLC) reveals nearly identical land-coverage patterns for both NIR and SWIR bands (See Figure 4). As Figure 4 shows, the majority of lithic mulching takes place just below the center of the image, and continues from the coast to the image-edge. MLC was performed on two different composites of SWIR (RGB 523 and RGB 614), and the results were similar. Further testing was continued on RGB 614 which reveals more distinctions between rocks and soil. Both images also manage to distinguish between mulch rocks, bedrock, and dry rocky soil, but SWIR is slightly more accurate in distinguishing between the different types of rock. Despite a 6.26 meter spatial resolution difference, the SWIR classification is almost identical to the NIR classification, and comparable in its accuracy. The difference between the two classifications was statistically insignificant as determined by a two-sample z-test ($z = 0.46$, $p > 0.05$).

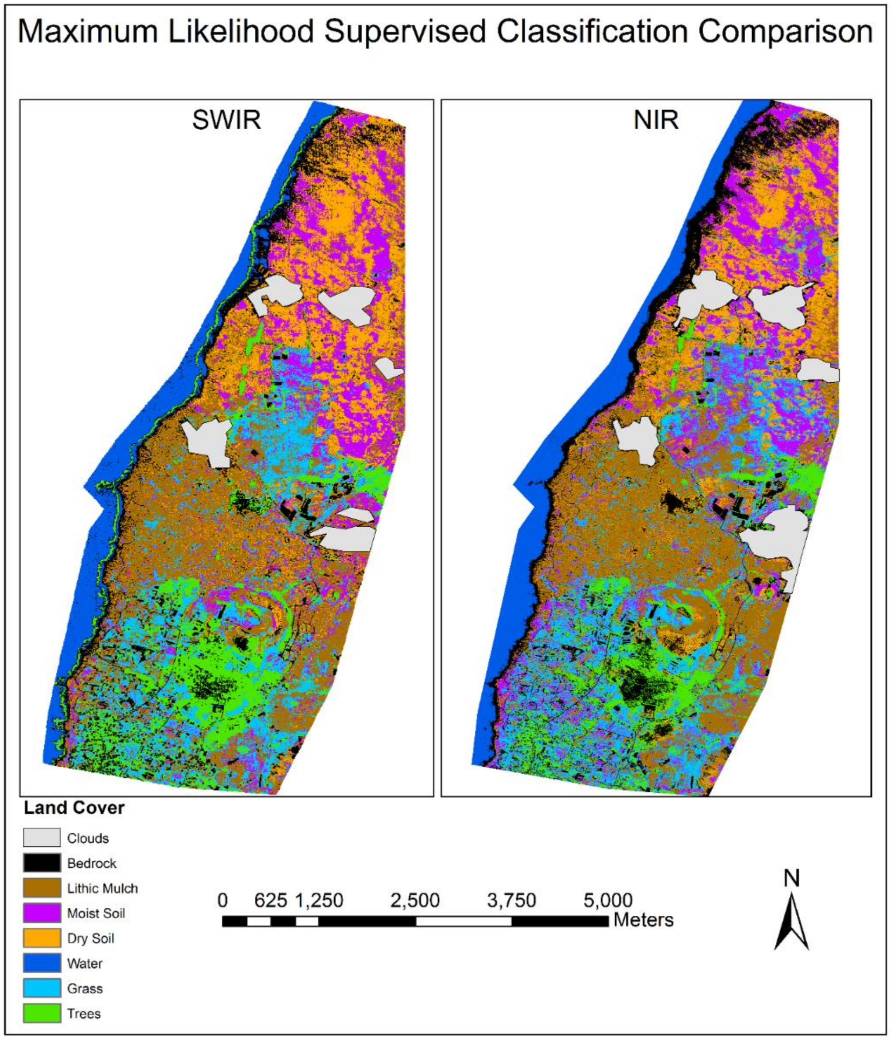

Figure 4. Maximum Likelihood Supervised Classification yielded nearly identical maps for both SWIR and NIR imagery. SWIR appears better and distinguishing between soil and rock, and better reveals flow marks for bedrock outcrops.

Accuracy

In order to determine whether or not SWIR is more accurate than NIR, several accuracy tests were conducted. For this study, five different assessment types are utilized: *diagonal sum*, *user's accuracy, producer's accuracy, kappa coefficient (κ)*, and the *Classification Success Index (CSI)*. Diagonal Sum (or overall accuracy) is one of the simplest measurements of association between two datasets (i.e. ground map and classified map) (Kuzera & Pontius Jr., 2008, p. 261;

Liu, et al., 2007, p. 607). The diagonal sum assessment produced 78.17% accuracy for NIR and 75.95% accuracy for SWIR. The results of the diagonal sum assessment are listed in Tables 3 and 4 below.

User's accuracy is the probability that a classified pixel represents that same classification on the ground, and *producer's accuracy* is the likelihood that a pixel is classified correctly (Liu, et al., 2007, p. 607). The overall user's accuracy (A) is calculated as:

$$A = \sum_{1}^{i} ua_i$$

where *i* is the total number of classes, and *ua* is the user's accuracy for each individual class. The overall producer's accuracy is calculated the same way, just replacing *ua* with the producer's accuracy (*pa*) for each class:

$$\square = \sum_{1}^{i} pa_i.$$

When calculating these accuracy measurements for the NIR imagery, the overall user's accuracy is calculated as 75.38% and the overall producer's accuracy is calculated as 76.16%. For SWIR imagery, the overall user's accuracy is 73.16% and the overall producer's accuracy is 73.28% (see Tables 4, 5, and 6). What is noticeable about these calculations, is that the overall user's and producer's classification accuracies are nearly identical, and the difference in the overall producer's and user's accuracy of NIR and SWIR are very small. This is even more impressive given the significant differences between the spatial resolutions of the two images.

Next, kappa (κ) coefficients were calculated to determine the level of statistical accuracy of the classifications. Calculating κ for the NIR classification yields a value of κ = 0.7418 and for SWIR classification κ = 0.7160 (see Table 6). K values between 0.61 and 0.80 are considered to

have substantial agreement (Landis & Koch, 1977, p. 165). This means that the κ coefficient suggests an exceptionally accurate classification for both the SWIR and NIR images.

CSI gives an overall assessment of classification effectiveness for a given image (see Koukoulas and Blackburn 2001). CSI is a good accuracy test to use if the goal of the analysis is to classify a large area with many equally important land cover classes (Owji, et al., 2014, p. 1493). As such, CSI values can reveal the map or image with the most accurate classifications. Koukoulas and Blackburn (2001) define the formula for CSI as:

$$CSI = (1 - (\frac{\sum_{i=1}^{n} ce_i + oe_i}{n})) \times 100$$

where *i* is the number of classes, *ce* is the error of commission for a specific class, and *oe* is the error of omission for a specific class. CSI provides "a thorough overall assessment of classification accuracy for all classes" (Koukoulas & Blackburn, 2001, p. 510) and CSI values of 80% or greater are considered to be indicators of successful classification, with lower values indicating some problems in the classification process. CSI testing on NIR imagery for this study yielded 66.69% accuracy, and SWIR yielded 60.39% accuracy. Thus, the CSI reveals that there are some substantial issues in the classification for both sets of imagery (largely due to very small spectral differences between classes). Classification for SWIR was further limited by its lower spatial resolution (7.5m).

The last step in the accuracy assessment is determining whether or not the difference between the SWIR and NIR classifications is statistically significant. In order to compare the two datasets, a two-sample z-test was used. The results of this significance test indicate that the difference between the classifications is *not* statistically significant ($z = 0.46$, $p > 0.05$).

All of these accuracy tests show that the classification process yields adequate classifications (see Table 6), with some errors clearly present (highlighted by CSI). With

substantially high user's accuracy, producer's accuracy, and overall accuracy, classifications are successful, further emphasized by the κ coefficients. Furthermore, the differences in the accuracies between NIR and SWIR are *not* statistically significant. Therefore, the accuracy comparisons show little difference between the two images in terms of classification accuracy.

Table 3: Error Matrix for NIR Classification

Land Classification	Grass	Water	Bed-rock	Trees	Moist Soil	Mulch	Dry Soil	Total	User's Accuracy
Grass	**19**	0	0	0	0.5	1	0.5	21	90.48%
Water	0	**8**	0	0	0	0	0	8	100.00%
Bedrock	0	0	**18.75**	0	0	0.75	0.5	20	93.75%
Trees	4	0	0	**15**	0	0.5	0.5	20	75.00%
Moist Soil	0.5	0	0	0	**17**	6	2.5	26	65.38%
Mulch	0	0	2	0	1	**20.5**	1.5	25	82.00%
Dry Soil	0.5	0	1.5	0	3.5	5.5	**19**	30	63.33%
Total Classified Points	24	8	22.25	15	22	34.25	24.5	150	-
Producer's Accuracy	79.17%	100%	84.27%	100%	77.27%	59.85%	77.55%	-	**78.17%**

Table 4: Error Matrix for SWIR Classification

Land Classification	Grass	Water	Bed-rock	Trees	Moist Soil	Mulch	Dry Soil	Total	User's Accuracy
Grass	**16.25**	0	0	2	1.25	1	0.5	21	77.38%
Water	0	**8**	0	0	0	0	0	8	100.00%
Bedrock	0	1.5	**17.5**	0	0	1	0	20	87.50%
Trees	1.33	0	0	**16.33**	0.5	1.84	0	20	81.65%
Moist Soil	1	0	0	1	**17**	5.5	1.5	26	65.38%
Mulch	1	0	1	0	1	**20.84**	1.16	25	83.36%
Dry Soil	1	0	1	0	4	6	**18**	30	60.00%
Total Classified Points	20.58	9.5	19.5	19.33	23.75	36.18	21.16	150	-
Producer's Accuracy	78.96%	84.21%	89.74%	84.48%	71.58%	57.60%	85.07%	-	**75.95%**

Table 5: SWIR Error

Land Classification	Grass	Water	Bedrock	Trees	Moist Soil	Mulch	Dry Soil
Omission Error	21.04 %	15.79 %	10.26%	15.52%	28.42%	42.40 %	14.93%
Commission Error	22.62 %	0.00%	12.50%	18.35%	34.62%	16.64 %	40.00%

Table 6: Classification Accuracy Test Comparisons

Accuracy Test	NIR	SWIR	Difference	Flaws (2010)	Ladefoged et. al. (2013)
Diagonal Sum	78.17%	75.95%	2.22%	65.23%	61.2%
User's Accuracy	81.42%	79.33%	2.09%	-	-
Producer's Accuracy	82.59%	78.81%	3.78%	-	-
Unweighted Kappa Coefficient	0.7418	0.7160	0.0258	.2425	.14
Classification Success Index	66.69%	60.39%	6.30%	-	-

Discussion

The classification of WorldView-3 imagery proved successful for both the NIR and SWIR bands. The variance between the two classifications was insignificant despite a 6.26 meter spatial resolution difference between the two images. For almost every class, the SWIR was nearly identical in accuracy to the NIR bands. If in the future, spatial resolution of SWIR is permitted at higher resolutions for commercial use, it may prove to be more accurate than the current NIR bands.

When using unsupervised classification, it was notable that SWIR produced a greater number of classes than the NIR, capturing subtle differences in moisture content between different pixels. Additionally, the unsupervised classification revealed linear striations in the landscape, which turned out to be bedrock and the remnants of ancient lava flows. As Hamilton, et al. (2011: 173) states, "[f]rom many places, the surface of the island appears as uninterrupted black and green. The black here consists mostly of the dark grey or very dark brown, weathered surfaces of

its flow lavas, extruded at different times from all three of the island's principal volcanoes." Nonetheless, unsupervised classification was less useful overall, due to some confusion in the items being classified.

Using supervised classification, better results were obtained, and a clear difference is noted in the classifications between lithic mulch and natural bedrock. When comparing the results of the WorldView-3 classifications to the study of Flaws (2010), differences are clearly noticeable between areas marked by Flaws (2010, p. 42) as high-density mulch locations and areas determined by this study to be natural bedrock (see Figure 5). SWIR proves to be effective at picking up moisture differences in the soil, and distinguishing between bedrock and lithic mulch.

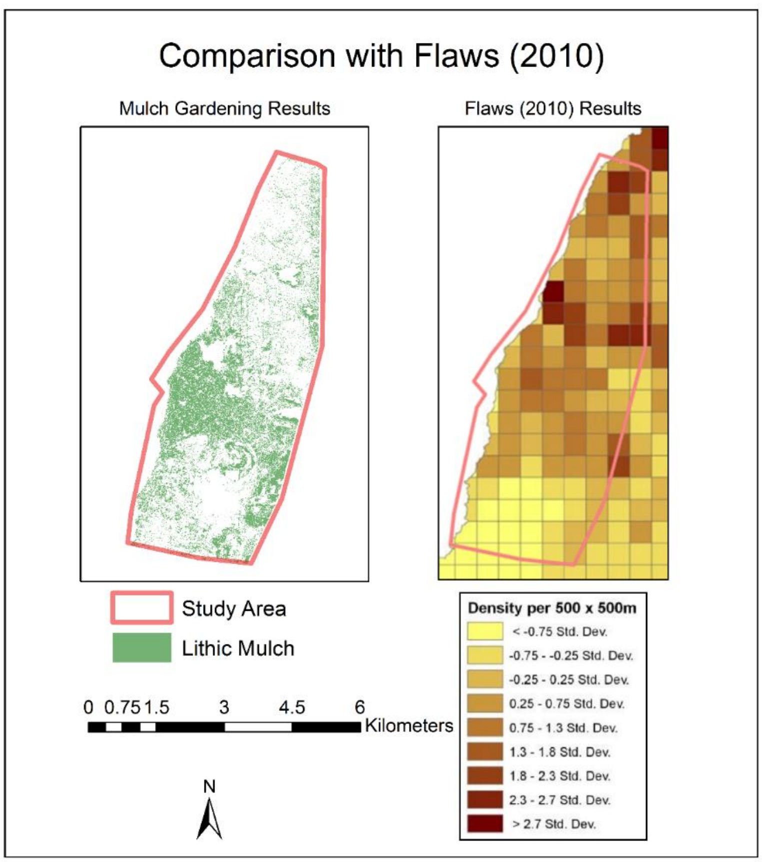

Figure 5. The map compares the results of the SWIR supervised classification of lithic mulching with Flaws' (2010) study of lithic mulching. Differences are noticeable, especially on the northernmost region of the study area, where density testing by Flaws reveals high concentrations

of lithic mulching, whereas this study determines that the area is composed of largely natural bedrock and not lithic mulch.

The supervised classification maps also prove that lithic mulch increases soil moisture, as areas between lithic mulch have higher amounts of vegetation and increased moisture content than areas without the lithic mulch. This adds to the evidence that mulch gardening was an important adaptation by the local population, and evolutionarily advantageous for survival in a challenging environmental setting. The results of both the SWIR and NIR show little difference and relatively accurate classifications. Therefore, SWIR can be considered to be comparable to NIR, despite a significantly lower spatial resolution. Future studies should employ both NIR and SWIR bands in order to capture all of the subtle differences in the landscape being studied, as well as the detail missed by the lower resolution images.

Conclusion

The results of this study show that 7.5 meter spatial resolution SWIR imagery is comparable in its accuracy to 1.24 meter spatial resolution NIR imagery. SWIR proves successful in distinguishing between natural rock outcrops and anthropogenically altered lithic mulch gardens; this is an area that should be further researched. In future archaeological remote sensing studies, both NIR and SWIR bands should be employed for landscape analyses.

This article has shown that the recently available high-resolution SWIR imagery from WorldView-3 is a valuable tool for archaeological studies. Although only 14.5% of the island's area was covered in this study, future work can certainly expand on the progress made here to cover the entire land-area of Rapa Nui, thus giving a true representation of land-use patterns throughout the island. In the future, if SWIR imagery is released to the public at a higher spatial resolution, it will likely be more accurate than NIR imagery for land-classification, especially in

terms of rock and mineral differentiation. More work is needed on the benefits of high-resolution SWIR imagery, but the results of this study are promising for future archaeological research.

References

Asadzadeh, S., & de Souza Filho, C. R. (2016). Investigating the capability of WorldView-3 superspectral data for direct hydrocarbon detection. *Remote Sensing of Environment, 173,* 162-173.

Asner, G. P., & Lobell, D. B. (2000). A biogeophysical approach for automated SWIR unmixing of soils and vegetation. *Remote Sensing of Environment, 74*(1), 99–112.

Basener, W., Brooks, B., Radin, M., & Wiandt, T. (2008). Rat instigated human population collapse on Easter Island. *Nonlinear Dynamics, Psychology, and Life Sciences, 12*(3), 227-240.

Blackburn, S. K. (2001). Introducing new indices for accuracy evaluation of classified images representing semi-natural woodland environments. *Photogrammetric Engineering and Remote Sensing, 67*(4), 499-510.

Bork, H.-R., Mieth, A., & Tschochner, B. (2004). Nothing but stones? A review of the extent and technical efforts of prehistoric stone mulching on Rapa Nui. *Rapa Nui Journal, 18*(1), 10-14.

Bradford, I. (2005). *Archaeological surveying with satellite imagery: Mapping subsistence features on Rapa Nui using remote sensing techniques.* MA Thesis, California State University, Long Beach , Anthropology.

Bradford, I., Lipo, C. P., & Hunt, T. L. (2005). An application of high-resolution satellite imagery for the mapping of habitation and subsistence features on Rapa Nui (Easter Island). *The Renaca Papers: VI International Conference on Rapa Nui and the Pacific* (pp. 113-123). Los Osos: Easter Island Foundation and University of Valparaiso.

Commendador, A. S., Dudgeon, J. V., Finney, B. P., Fuller, B. T., & Esh, K. S. (2013). A stable isotope (δ13C and δ15N) perspective on human diet on rapa nui (Easter Island) ca. AD 1400–1900. *American Journal of Physical Anthropology, 152*(2), 173-185.

Congalton, R. G. (1991). A review of assessing the accuracy of classifications of remotely sensed data. *Remote Sensing of Environment, 37*(1), 35-46.

Digital Globe. (2014). WorldView-3 Datasheet. Retrieved March 13, 2016, from http://www.spaceimagingme.com/downloads/sensors/datasheets/DG_WorldView3_DS_2014.pdf

Drake, N. A., Mackin, S., & Settle, J. J. (1999). Mapping vegetation, soils, and geology in semiarid shrublands using spectral matching and mixture modeling of SWIR AVIRIS imagery. *Remote Sensing of Environment, 68*(1), 12-25.

Driggers, R. G., Hodgkin, V., & Vollmerhausen, R. (2013). What good is SWIR? Passive day comparison of VIS, NIR, and SWIR. *SPIE Defense, Security, and Sensing, 8706*, 87060L-2 - 87060L-15.

Fischer, S. R. (2005). *Island at the end of the world: The turbulent history of Easter Island.* London: Reaktion Books.

Flaws, A. L. (2010). *The identification and analysis of Rapa Nui (Easter Island) rock gardens by satellite remote sensing.* MA Thesis, University of Auckland, Anthropology.

Freedman, D., Pisani, R., & Purves, R. (2007). *Statistics* (4th ed.). New York: W. W. Norton and Company.

Gill, T. K., & Phinn, S. R. (2008). Estimates of bare ground and vegetation cover from Advanced Spaceborne Thermal Emission and Reflection Radiometer (ASTER) short-wave-infrared reflectance imagery. *Journal of Applied Remote Sensing, 2*(1), 023511. doi:10.1117/1.2907748

Horrocks, M., & Wozniak, J. A. (2008). Plant microfossil analysis reveals disturbed forest and a mixed-crop, dryland production system at Te Niu, Easter Island. *Journal of Archaeological Science, 35*(1), 126-142.

Hunt, T., & Lipo, C. (2012). *The statues that walked: Unraveling the mystery of Easter Island.* Berkeley: Counterpoint.

Jensen, J. R. (2007). *Remote sensing of the environment: An Earth resource Perspective* (2nd ed.). Upper Saddle River, NJ: Prentice Hall.

Kruse, F. A., Baugh, W. M., & Perry, S. L. (2015). Validation of DigitalGlobe WorldView-3 Earth imaging satellite shortwave infrared bands for mineral mapping. *Journal of Applied Remote Sensing, 9*(1), 096044. doi:10.1117/1.JRS.9.096044

Kuzera, K., & Pontius Jr., R. G. (2008). Importance of matrix construction for multiple-resolution categorical map comparison. *GIScience & Remote Sensing, 45*(3), 249–274.

Ladefoged, T. N., Flaws, A., & Stevenson, C. M. (2013). The distribution of rock gardens on Rapa Nui (Easter Island) as determined from satellite imagery. *Journal of Archaeological Science, 40*, 1203-1212. doi:10.1016/j.jas.2012.09.006

Ladefoged, T. N., Stevenson, C. M., Haoa, S., Mulrooney, M., Puleston, C., Vitousek, P. M., & Chadwick, O. A. (2010). Soil nutrient analysis of Rapa Nui gardening. *Archaeology in Oceania, 45*(2), 80-85.

Landis, J. R., & Koch, G. G. (1977). The measurement of observer agreement for categorical data. *Biometrics, 33*(1), 159-174.

Lightfoot, D. R. (1994). Morphology and ecology of lithic-mulch agriculture. *Geographical Review, 84*(2), 172-185.

Lipo, C. P., & Hunt, T. L. (2005). Mapping prehistoric statue roads on Easter Island. *Antiquity, 79*(303), 158-168.

Liu, C., Frazier, P., & Kumar, L. (2007). Comparative assessment of the measures of thematic classification accuracy. *Remote Sensing of Environment, 107*(4), 606–616.

Longbotham, N. W., Pacifici, F., Malitz, S., Baugh, W., & Camps-Valls, G. (2015). Measuring the spatial and spectral performance of WorldView-3. *Hyperspectral Imaging and Sounding of the Environment* (pp. HW3B-2). Optical Society of America.

Longbotham, N., Pacifici, F., Baugh, B., & Camps-Valls, G. (2014). “Prelaunch Assessment of WorldView-3 Information. *IEEE Workshop on Hyperspectral Image and Signal Processing.* Whispers.

Louwagie, G., Stevenson, C. M., & Langohr, R. (2006). The impact of moderate to marginal land suitability on prehistoric agricultural production and models of adaptive strategies for Easter Island (Rapa Nui, Chile). *Journal of Anthropological Archaeology, 25*(3), 290–317.

Maglione, P. (2016). Very High Resolution Optical Satellites: An overview of the most commonly used. *American Journal of Applied Sciences*, *13*(1), 91-99.

Mann, D., Edwards, J., Chase, J., Beck, W., Reanier, R., Mass, M., Loret, J. (2008). Drought, vegetation change, and human history on Rapa Nui (Isla de Pascua, Easter Island). *Quaternary Research, 69*(1), 16-28.

Martinsson-Wallin, H., & Wallin, P. (2014). Spatial perspectives on ceremonial complexes: Testing traditional land division on Rapa Nui. In H. Martisson-Wallin, & T. Thomas (Eds.), *Monuments and people in the Pacific* (pp. 317-342). Uppsala: Uppsala University.

Mieth, A., & Bork, H.-R. (2015). Degradation of resources and successful land-use management on prehistoric Rapa Nui: Two sides of the same coin. In N. Cauwe, & M. D. Dapper (Eds.), *Easter Island. Collapse or Transformation? A State of the Art. Proceedings of the International Conference of Brussels (9-10/11/2012)* (pp. 91-113). Brussels: Royal Academy for Overseas Sciences.

Morrison, A. E. (2012). *An archaeological analysis of Rapa Nui settlement structure: A multi-scalar approach.* PhD Dissertation, University of Hawai'i at Manoa.

Owji, A., Boroujeni, I. E., Kamali, A., Hosseinifard, S. J., & Bodaghabadi, M. B. (2014). The effects of hydrometer reading times on the spatial variability of soil textures in southeast Iran. *Arabian Journal of Geosciences, 7*(4), 1491-1499.

Parcak, S. H. (2009). *Satellite Remote Sensing for Archaeology.* New York: Routledge.

Parcak, S., Gathings, D., Childs, C., Mumford, G., & Cline, E. (2016). Satellite evidence of archaeological site looting in Egypt: 2002–2013. *Antiquity, 90*(349), 188-205.

Pontius Jr, R. G., & Millones, M. (2011). Death to Kappa: birth of quantity disagreement and allocation disagreement for accuracy assessment. *International Journal of Remote Sensing, 32*(15), 4407-4429.

Rainbird, P. (2002). A message for our future? The Rapa Nui (Easter Island) ecodisaster and Pacific island environments. *World Archaeology*, *33*(3), 436-451.

Reitz, E. J., Newsom, L. A., Scudder, S. J., & Scarry, C. M. (2008). Introduction to environmental archaeology. In E. J. Reitz, C. M. Scarry, & S. J. Scudder (Eds.), *Case Studies in Environmental Archaeology* (2nd ed., pp. 3-20). Springer.

Sahlins, M. D. (1955). Esoteric efflorescence in Easter Island. *American Anthropologist, 57*(5), 1045-1052.

Stevenson, C. M., Jackson, T. L., Mieth, A., Bork, H.-R., & Ladefoged, T. N. (2006). Prehistoric and early historic agriculture at Maunga Orito, Easter Island (Rapa Nui), Chile . *Antiquity, 80*, 919–936.

Stevenson, C. M., Ladefoged, T. N., & Haoa, S. (2002). Productive strategies in an uncertain environment: prehistoric agriculture on Easter Island. *Rapa Nui Journal, 16*(1), 17-22.

Stevenson, C. M., Wozniak, J., & Haoa, S. (1999). Prehistoric agricultural production on Easter Island (Rapa Nui), Chile. *Antiquity, 73*(282), 801-812.

Vargas, P., Cristino, C., & Izaurieta, R. (2007). GIS applications in Easter Island: Geodetic adjustments and survey maps accuracy. In S. McLaughlin (Ed.), *The Gotland Papers: Selected Presentations from the VII International Conference on Easter* (pp. 87-93). Gotland University Press.

Wozniak, J. A. (1999). Prehistoric horticultural practices on Easter Island: Lithic mulched gardens and field Systems. *Rapa Nui Journal, 13*(3), 95-99.

Wozniak, J. A. (2003). *Exploring landscapes on Easter Island (Rapanui) with geoarchaeological studies: Settlement, subsistence, and environmental changes.* PhD Dissertation, University of Oregon, Anthropology.